

THE EFFECT OF PRESSURE ON THE DEFECTS IN ALKALI HALIDE CRYSTALS

BY SHIGERU MINOMURA, KAZUO INOUE, KUNIO OZAWA
and MASATOMO FUJIMOTO

Introduction

The defects in crystals can be produced in appreciable concentration by means of mechanical work (compression, tension or bending), irradiation, and addition of chemical impurities. They have been observed directly by micrographic patterns of etched surfaces and x-ray diffraction patterns, and measured indirectly by electrical, optical, and other physical property changes.

The previous papers¹⁾ have shown from the observations of etch patterns, Laue patterns, and color centers that the plastic flow is caused in alkali halide crystals by the hydrostatic compression. Gilman and Johnston²⁾ have studied by thier micrographic observation the origin and growth of glide bands and the radiation damage in LiF crystal. Mayburg³⁾ has measured the pressure dependence on the low frequency dielectric constant of alkali halide crystals up to 8,000 bars, and shown that they are reduced with increasing pressure. Their reductions will be contributed by the inhibition of microscopic motion of charge particles of the substances.

The present study has shown that the natures and contributions of the defects in alkali halide crystals produced by the application of hydrostatic compression, cleavage, irradiation, and impurities are obtained by means of etching, x-ray diffraction, dielectric constant, and optical absorption.

Experimentals

Preparation of samples In this experiment the crystals of LiF, NaCl, NaI, KI, and NaI (Tl) and KI (Tl) which were activated with TlI of the content of about 0.2% were used. NaI and NaI(Tl) crystals were produced by Stockbarger's method⁴⁾ of lowering a pointed bottom crucible along the axis of vertical tubular furnaces. The other crystals were produced by the modification of Kyropoulos' method⁵⁾ of growing the cooling seed in the melt. The vacuum furnace which makes possible the production of the crystals by both the Stockbarger's and the Kyropoulos' methods was constructed for the prevention of hydrolysis of the melt in crystallization. The arrangement is shown in Fig. 1.

1) R. Kiyama and S. Minomura, *This Journal*, **27**, 43 (1957)

S. Minomura, *ibid.*, **24**, 28 (1954)

2) J. J. Gilman and W. G. Johnston, *Dislocations and Mechanical Properties of Crystals, An International Conference held at Lake Placid*, (1956), p. 116; *J. App. Phys.*, **29**, 877 (1958); **30**, 129 (1959)

3) S. Mayburg, *Phys. Rev.*, **79**, 375 (1950)

4) D. C. Stockbarger, *Disc. Farad. Soc.*, No. 5, *Crystal Growth*, 299 (1949)

5) S. Kyropoulos, *Z. anorg. Chem.*, **154**, 308 (1926)

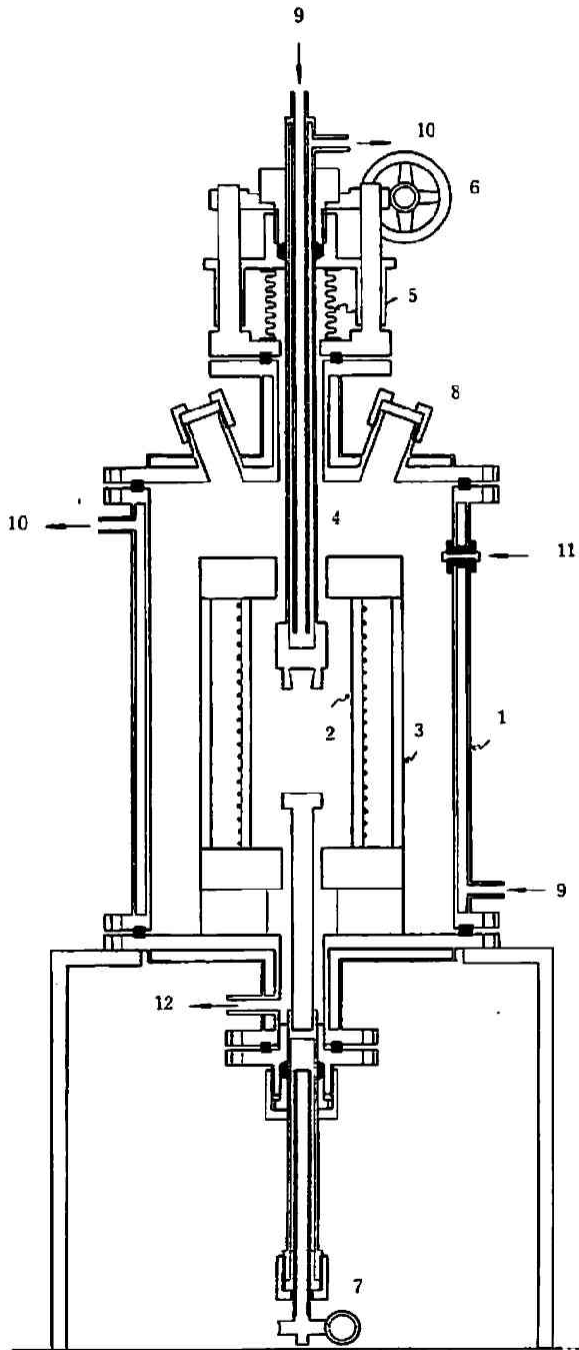


Fig. 1 The vacuum furnace for Stockbarger's and Kyropoulos' methods of crystallization from melt

- 1: 1-m-diameter steel pipe
- 2: heater
- 3: radiation baffle
- 4: cooler
- 5: bellow
- 6: raising controller
- 7: lowering controller
- 8: window
- 9: water inlet
- 10: water outlet
- 11: power connection
- 12: to vacuum pump

The experimental samples were prepared by cleaving thin specimens from large single crystals, usually about $16 \times 12 \text{ mm}^2$ in area and $0.8 \sim 1.6 \text{ mm}$ thick. The faces of the cleaved specimens were (100) planes.

The irradiation to crystals were performed by γ -rays ($2.2 \times 10^5 \text{ r/hr}$) from Co^{60} of 2,400 Curie in Chemical Institute of Kyoto University, electrons ($3 \times 10^5 \text{ rad/sec}$) from Van de Graaf of 1.75 Mev and $50 \mu\text{A}$ in Osaka Institute of Japanese Association for Radiation Research on Polymers, and neutrons ($10^{11} \text{ n/cm}^2\text{sec}$) from JRR-1 of 35 KW in Japanese Atomic Power Institute. The maximum exposures were $1.1 \times 10^7 \text{ r}$ in γ -rays, $1.5 \times 10^5 \text{ rad}$ in electrons, and $1.1 \times 10^{16} \text{ nvt}$ in neutrons.

Etching LiF crystal was polished in a 2-vol % aqueous solution of NH_4OH for an hour, and rinsed in alcohol and then in ether. This treatment removed about 80μ from the surface of a crystal. The polished crystal was etched for 30 to 60 seconds in the conc. mixed acids consisting of equal parts of HF, HNO_3 , and glacial acetic acid plus 1-vol % HNO_3 saturated with $\text{Fe}(\text{NO}_3)_3$. The etch was followed by an alcohol rinse and then an ether rinse.

NaCl crystal was polished for 20 seconds in a 40-vol % aqueous solution of alcohol, and rinsed in alcohol and then in ether. This treatment removed about 80μ from the surface of a crystal. The etch was performed for 60 to 90 seconds in glacial acetic acid, and followed by an alcohol rinse and then an ether rinse. The etched crystal was dried quickly with filter paper. The magnification of micrograph of etch pattern was $\times 100$ or $\times 400$.

Measurement of dielectric constant at high pressure The high pressure bomb with four electrodes and one stop valve which is connected to an intensifier was constructed. The schematic diagram is shown in Fig. 2. The main high pressure problem was to seal an electrical lead into the bomb. The sealing was performed by unsupported area principle. The high pressure electrode was satisfactory for measuring the dielectric constant up to $5,000 \text{ kg/cm}^2$. The resistance pressure gauge using manganin wire was designed for measuring pressure. The pressure fluid was silicone liquid.

The dielectric constant was measured with an impedance bridge of parallel resistance type at 1,000 c. p. s. Thin specimens of crystals covered with vaseline were held between guarded and unguarded electrodes, Al 30μ thick, which were stuck on plastic plates. Three electrical leads of 0.8 mm in diameter and 25 mm in length soldered with the electrodes acted both as electric connection to the high pressure electrodes and as supports. The actual geometry is shown in Fig. 2.

The dielectric constants at atmospheric pressure of alkali halide crystals obtained from this measurement coincide with those in American Institute of Physical Handbook in 1957 within the experimental error. The pressure dependence of the dielectric constants can be reproduced. However, it might be changed by using an electrode gold-plated on the crystal³⁾.

X-ray diffraction and infrared absorption The effect of irradiation on the mosaic-structure and the lattice constant of LiF and NaCl crystals was studied by means of x-ray diffraction patterns by the Laue and Bragg methods, which were obtained by means of a Shimadzu Geiger

6) R. Kiyama and S. Minomura, *This Journal*, 23, 10 (1953)

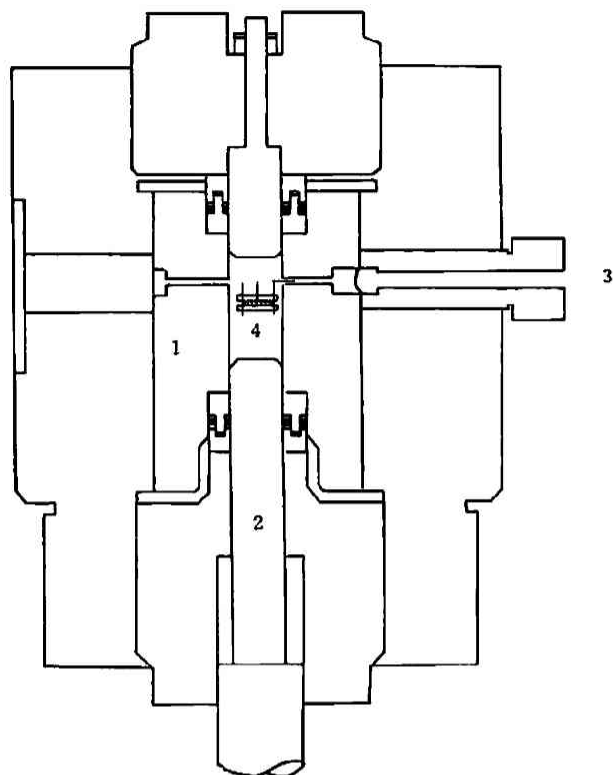


Fig. 2 The pressure bomb for dielectric measurement

- 1: pressure-proof cylinder of 20mm inner diameter
- 2: moving piston connected to intensifier
- 3: electrode
- 4: sample

counter x-ray diffractometer.

The irradiation effect on anion complex in LiF crystal was studied by means of infrared absorption spectra, which were obtained by the Perkin-Elmer Model 21 infrared spectrophotometer equipped with NaCl prism.

Results and Discussions

Etch patterns The low-angle tilt boundaries and the dislocation half loops are etched on the cleavage crack in an as-grown LiF crystal. This is shown in Fig. 3 (a). The tilt angles of the boundaries are $0.5 \sim 1.5$ seconds. The dislocation density given by the etchpits is $10^3 \sim 10^4$ disl./cm². The slip traces of both the edge and screw dislocations are etched by the hydrostatic compression at $7,500 \text{ kg/cm}^2$. Fig. 3 (b) and (c) show them on the polished and the cleaved surfaces of the crystal. The edge orientations of $(110) [1\bar{1}0]$ dislocations make an angle of 45 degrees with the cube edges. The screw orientations are parallel to those. The dislocation densities are $\sim 10^2$ disl./cm². The uniformity of the dislocation motion can be seen by the treatment of cleavage, etching, bending, and re-etching, in Fig. 3 (b). The tiny etchpits having a sharp pyramidal shape constitutes the dislocation half loops multiplied by bending, and the larger etchpits having a coarse flat-bottomed pyramidal shape constitutes the original half loops.

Fig. 3

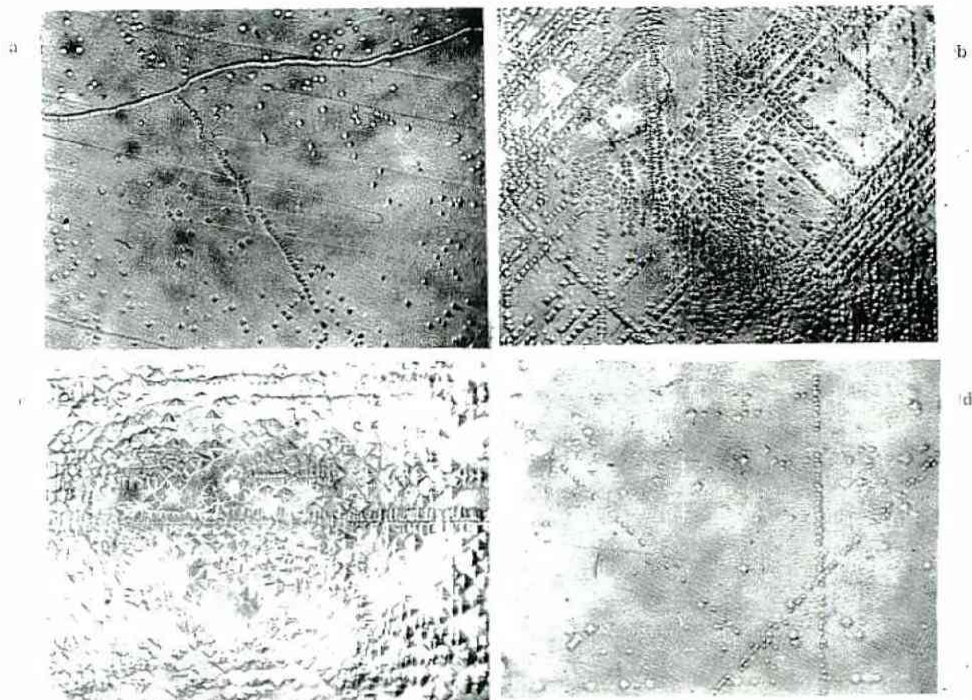


Fig. 4

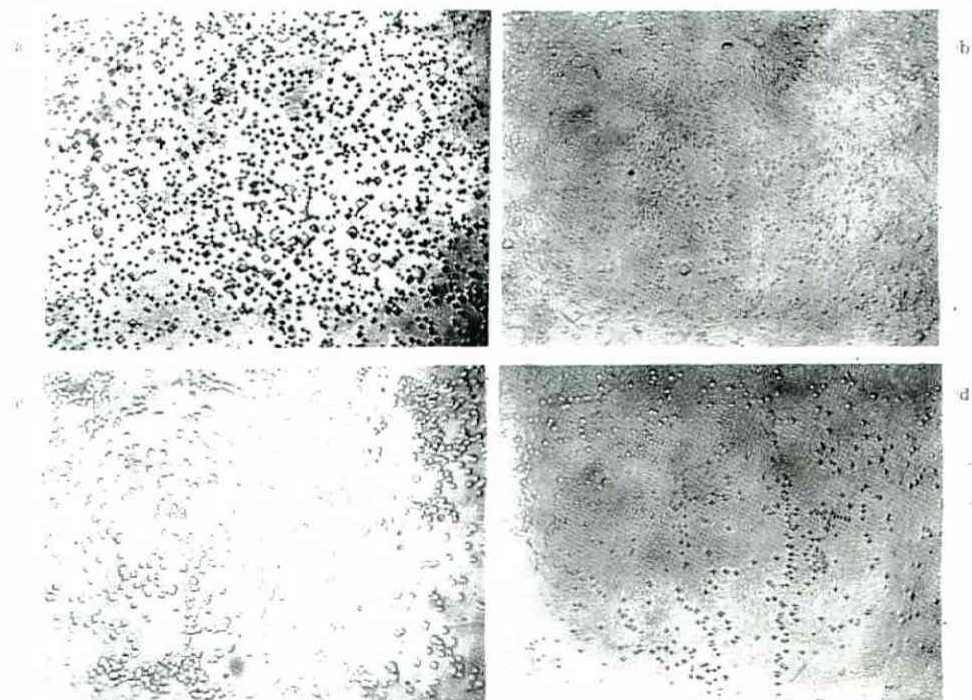


Fig. 3 Growth of glide bands in LiF by compression and bending ($\times 400$)
 (a), cleavage plane of as grown crystal; (b), (c), compressed at $7,500 \text{ kg/cm}^2$
 for 1 and 24 hours; (d), cleaved and bended and doubly etched.

Fig. 4 Etch patterns in irradiated and polished LiF and NaCl crystals ($\times 400$)
 (a), 1.2×10^7 rad electron irradiated LiF; (b) 1.1×10^7 r γ -rays irradiated LiF;
 (c), 6.6×10^5 r γ -rays irradiated NaCl; (d), 3.6×10^{14} nvt neutron irradiated LiF.

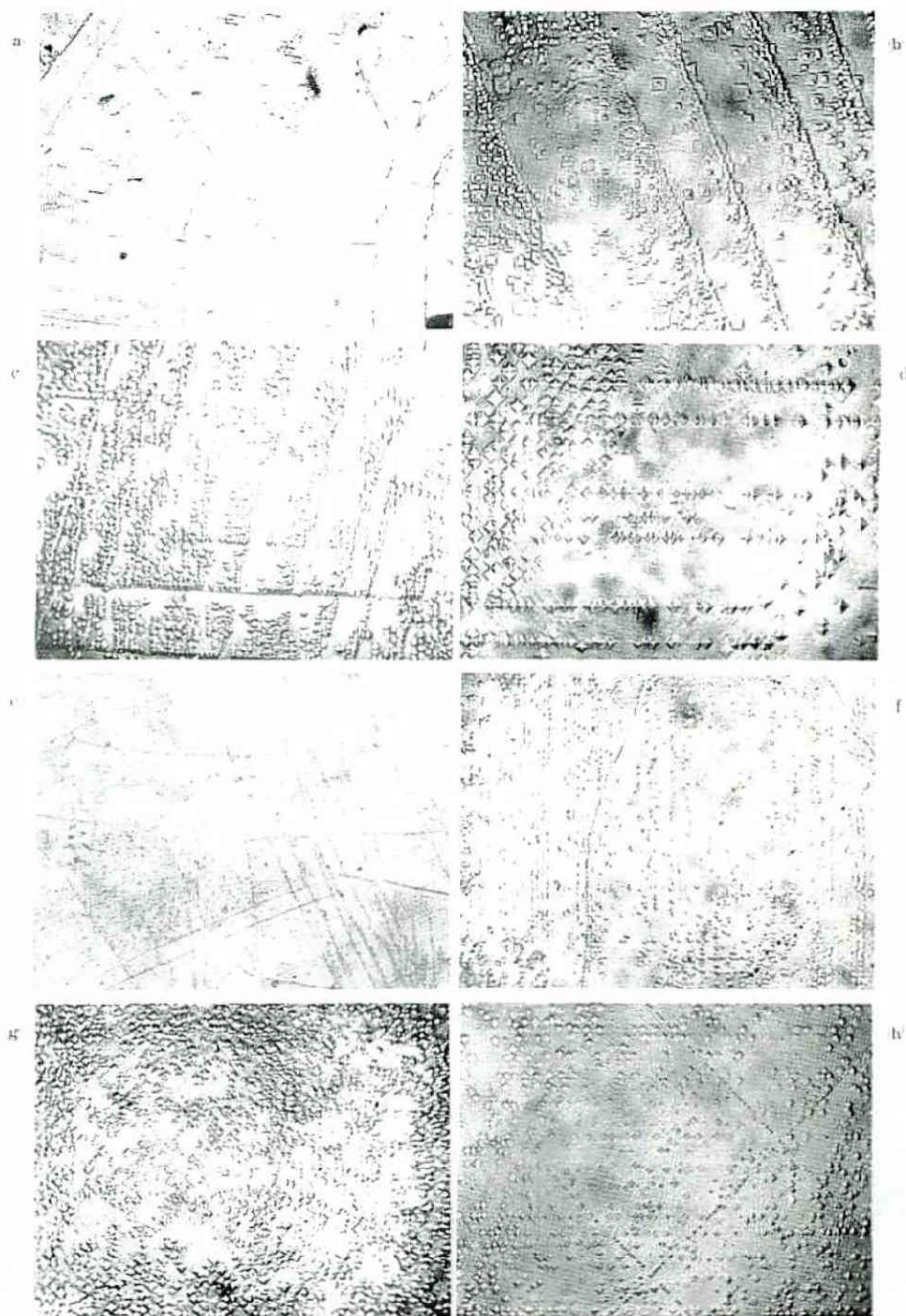


Fig. 5 Growth of glide bands in irradiated LiF and NaCl crystals by cleavage crack ; (a) and (e), $\times 100$; the others, $\times 400$

(a) and (c), 1.5×10^5 rad electron irradiated LiF ; (b), 1.5×10^5 rad electron irradiated NaCl ; (d), 1.2×10^7 rad electron irradiated LiF ; (e) and (f), 5.5×10^5 r γ -rays irradiated LiF ; (g), 1.1×10^{15} nvt neutron irradiated LiF ; (h), cleaved and bended and doubly etched LiF.

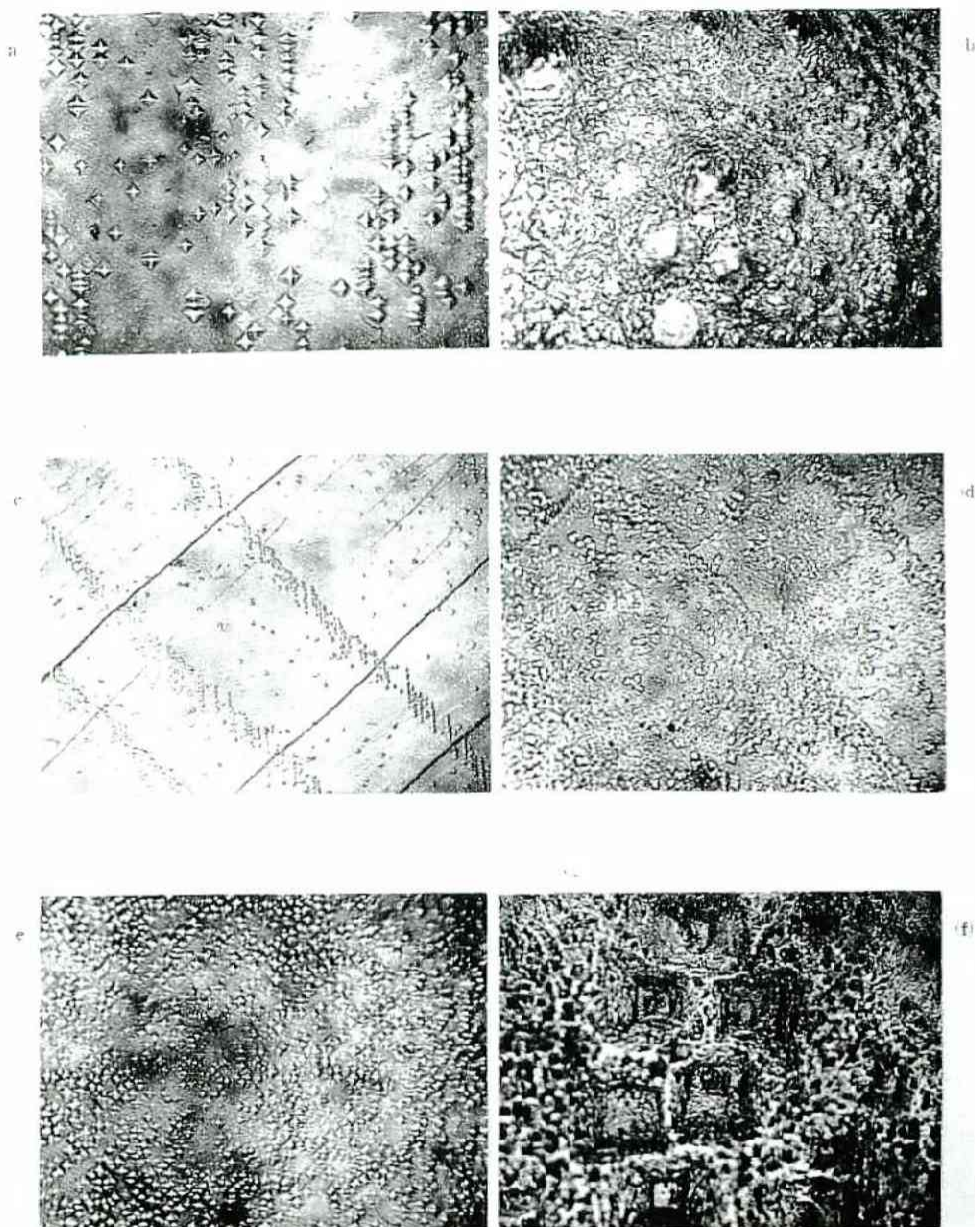


Fig. 6 Effect of annealing on etching structure of irradiated LiF crystal
 (a) and (b), 1.2×10^7 rad electron irradiated; (c) and (d), 6.6×10^5 r
 γ -rays irradiated; (e) and (f), 1.1×10^{16} nvt neutron irradiated.
 (a), (c) and (e), annealed at 450°C for 1 hour; (d), annealed at 550°C
 for 1 hour; (b) and (f), annealed at 700°C for 7 hours.

Fig. 7

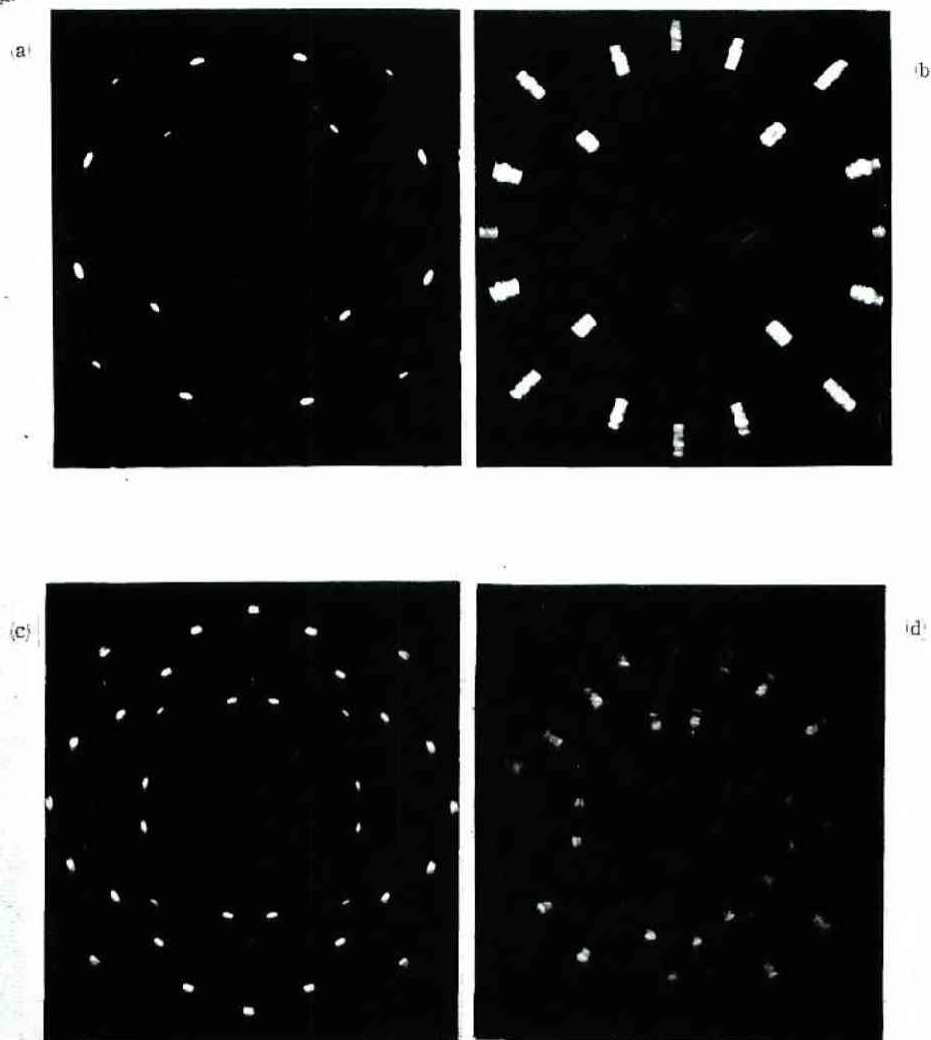


Fig. 8



Fig. 7 The effect of electron irradiation on Laue patterns from LiF and NaCl crystals (a), as-grown LiF, 3.0 mm thick; (b) 1.5×10^9 rad electron irradiated LiF, 7.6 mm thick; (c), as-grown NaCl, 3.0 mm thick; (d), 1.5×10^9 rad electron irradiated NaCl, 5.8 mm thick.

Fig. 8 Crack tips produced in 1.5×10^9 rad electron irradiated LiF crystal ($\times 135$)

It is shown by the etch patterns on the polished surfaces of the crystals that the defect aggregations are produced by 1.2×10^7 rad electron exposure (Fig. 4 (a), LiF), and 1.1×10^7 r γ -rays exposure (Fig. 4 (b), LiF), and 6.6×10^5 r γ -rays exposure (Fig. 4 (c), NaCl), and 3.6×10^{14} nvt neutron exposure (Fig. 4 (d), LiF). The aggregations are constituted by two or three etchpits and distribute at random. The uniform roughening of the etched surfaces is made by neutron exposure greater than $\sim 10^{15}$ nvt. The axes of their aggregations are aligned mostly along (110) $[\bar{1}\bar{1}0]$ dislocations. It seems likely to etch small dislocation half loops.

The effects of cleavage crack on the etch patterns are shown in Fig. 5 (a)~(g). The glide bands constituted by small half loops aligned in parallel to the cube edges are given by the application of the stress pulse. The orientations of the shock front, which starts from the lower right corner in Fig. 5 (a), do not always spread in parallel to the edge dislocations, but tend to align in the orientations of the dislocations, Fig. 5 (d). The defect-free zones are left between the glide bands. Some patterns show polygonization structure of dislocations, Fig. 5 (f). The etch patterns produced by neutron exposures are not affected by cleavage crack, Fig. 5 (g). This suggests the defects by neutron exposure must be bound in the crystal lattice more stably than those by electron or γ -ray exposure.

The etch pattern similar to the glide bands on the cleaved surfaces of the irradiated crystals is obtained by the treatments of cleavage crack, bending, and double etching for LiF crystal, as in Fig. 5 (h). The new dislocations of tiny etchpits with high density aligned along the edge and screw orientations are produced by the dislocation motion and the multiplication of half loops during bending.

The effect of annealing at 450°C and 550°C for an hour and at 700°C for 7 hours in the vacuum furnace on the dislocation half loops produced by cleavage crack in irradiated LiF crystal are shown in Fig. 6 (a)~(f). The half loops become more coarse and less dense, and tend to align along the orientations of (110) $[\bar{1}\bar{1}0]$ dislocations. The etchpits by electron and neutron exposures grow upon annealing at 700°C, Fig. 6 (b) and (f). The fact that the etchpits decrease in the density and increase in the average volume upon annealing may suggest the aggregation of the defects and the loss of fluorine from the crystals.

X-ray diffraction patterns The spots of Laue patterns of LiF and NaCl crystals are changed into discontinuous asterism streaks by 1.5×10^3 rad electron exposure, as shown in Fig. 7 (a)~(d). The spread of misorientation determined by the length of the streaks is 1.5° for LiF crystal and 1.3° for NaCl crystal. The spots do not spread into arcs, which are mainly due to plastic curvature. The fact that many crack tips aligned along (110) $[\bar{1}\bar{1}0]$ dislocations are produced in the terminal region of the colored part of thick electron irradiated LiF crystal gives the evidences of local lattice expansion and compression, as shown in Fig. 8.

The first-order x-ray diffraction patterns by Bragg method from (200) planes of electron and neutron irradiated LiF crystals show not only the splitting of the misorientation of the substructure, but also the broadening of the half-width caused by lattice expansion, as in Fig. 9 which is showing the intensity of scattered beam *vs.* twice the angle of incident beam to the crystals, 2θ . The maximum splitting from the pattern at 45.02° for $\text{CuK}\alpha$ is 0.5° for 1.5×10^3 rad electron exposure, and 1.0° for $10^{14} \sim 10^{16}$ nvt neutron exposure. The broadening of the half-width is

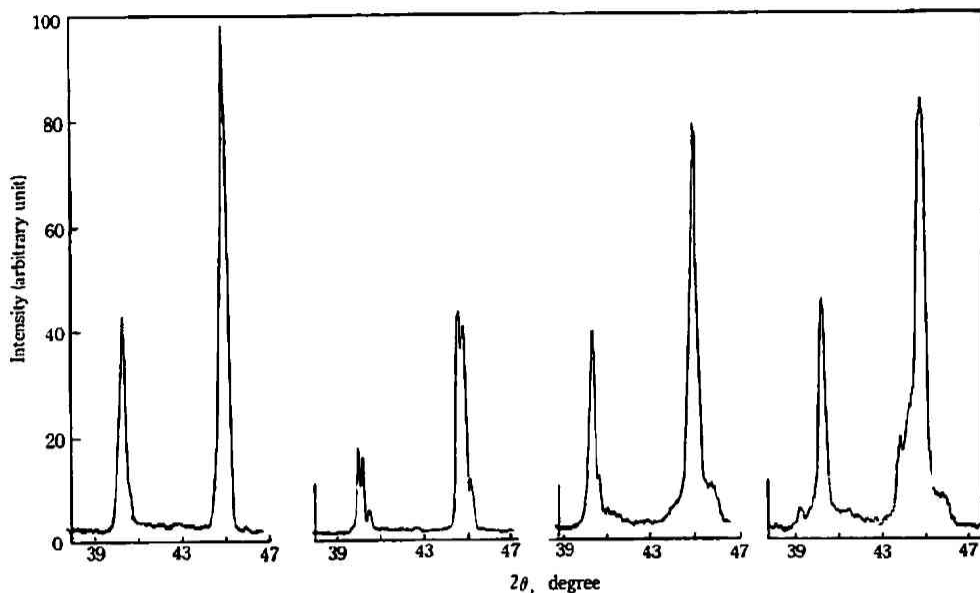


Fig. 9 The effect of electron and neutron irradiation on Bragg patterns from LiF crystal, (intensity vs. 2θ)

From the figure on the left;

- (a), as-grown crystal; (b), 1.5×10^8 rad electron irradiated;
 (c), 3.6×10^{14} nvt neutron irradiated; (d), 1.1×10^{16} nvt neutron irradiated

$0.33^\circ + 0.15^\circ$ for the electron exposure and $0.33^\circ + 0.17^\circ$ for the neutron exposure, where the half-width of the as-grown crystal is 0.33° .

Dielectric constant The pressure dependences of the dielectric constants of LiF, NaCl, NaI and KI crystals are shown in Fig. 10. The dielectric constants of LiF and NaCl crystals at atmospheric pressure are decreased by γ -ray, electron and neutron exposures, and those of NaI and KI crystals are increased by the addition of Thallous ions. The dielectric constants are reduced directly by increasing pressure. The pressure dependences of the dielectric constants, $-(\partial\epsilon/\partial P)_T \times 10^{-4} (\text{kg}/\text{cm}^2)^{-1}$, are listed in Table 1.

It can be concluded that the pressure dependences of the dielectric constants increase more

Table 1 The pressure dependences of the dielectric constants, $(\partial\epsilon/\partial P)_T \times 10^{-4} (\text{kg}/\text{cm}^2)^{-1}$, for four alkali halide crystals

NaCl		LiF		NaI		KI	
as-grown	1.12	as-grown	0.72	as-grown	2.67	as-grown	0.82
γ -ray irrad. (1.1×10^7 r)	2.37	electron irrad (1.5×10^8 rad)	1.50	NaI (Tl)	1.67	KI (Tl)	0.28
neutron irrad. (1.1×10^{16} nvt)	2.38						

The Effect of Pressure on the Defects in Alkali Halide Crystals

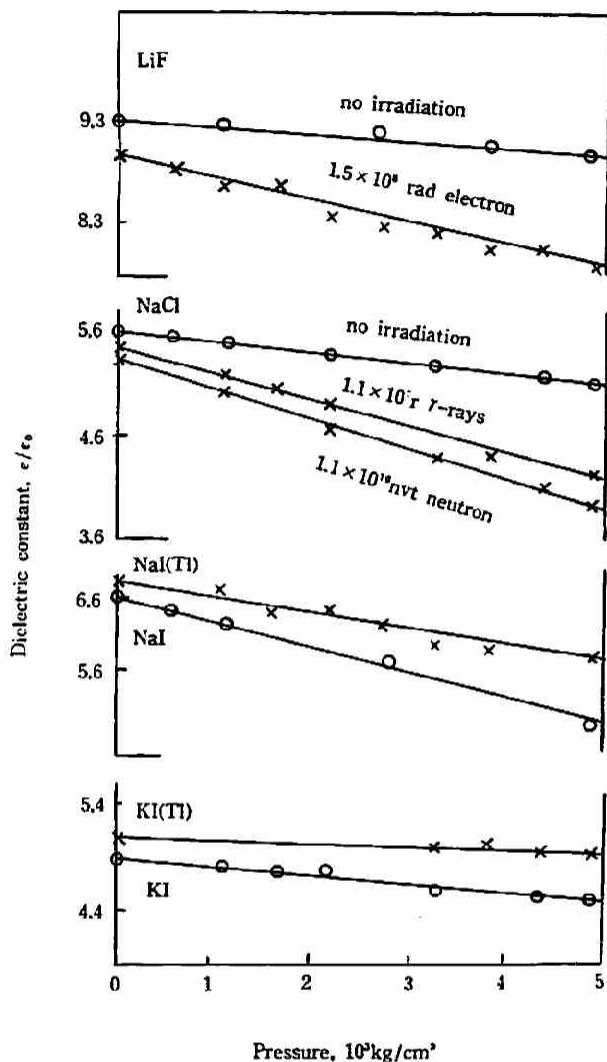


Fig. 10 The pressure dependence of the dielectric constants of alkali halide crystals irradiated by γ -ray, electron and neutron beams and activated by Thallous ions

rapidly in the irradiated crystals and decrease more slowly in the activated crystals than in the original crystals. Mott and Littleton⁷⁾ have derived the equation,

$$\frac{\epsilon - 1}{4\pi} = \frac{8\pi\beta\beta_0(\gamma - 1)/3 + (\beta + \beta_0)}{1 - 4\pi(\beta + \beta_0)/3 + 16\pi^2\beta\beta_0(1 - \gamma^2)/9} \quad (1)$$

where ϵ is the dielectric constant, β_0 is the polarizability of the electrons of the ions per unit volume, β is the ionic polarizability per unit volume and γ is the constant of the inner field. The value of the constant γ is defined as follows,

$$F = E + \gamma \frac{4}{3} \pi P, \quad (2)$$

where F is the effective polarizing field, E is the external electric field and P is the total polari-

7) N. F. Mott and M. J. Littleton, *Trans. Farad. Soc.*, 34, 485 (1938)

zation per unit volume. The relation between the ionic polarizability (β) and the repulsive overlap force constant (R) is

$$\beta = N(Ze)^2/R, \quad (3)$$

where Ze is the ionic charge, N is the number of ion pairs per unit volume. For the NaCl type lattice, the relation between the force constant (R) and external pressure (P) is

$$R = 6a/\alpha - 8Pa, \quad (4)$$

where a is the lattice constant and α is the compressibility. The increase of the external pressure makes the ionic polarizability (β) decrease from eq. (3), according to the increase of the force constant (R) from eq. (4). The decrease of the ionic polarizability (β) is ascribed to the decrease of the dielectric constant from eq. (1).

On the other hand, Yamashita⁸⁾ has derived the equation.

$$\frac{d\epsilon}{da} = -\frac{(e-1)(\epsilon+2)}{a} - \frac{8\pi}{E^2} \left[\frac{dA}{da} P_e^2 + \frac{dB}{da} P_e P_z + \frac{dC}{da} P_z^2 \right] \frac{1}{2a^3}, \quad (5)$$

where P_z is dipole moment caused by the displacement of ion pairs, P_e is dipole moment caused by the distortion of a negative ion. A, B, C are parameters depending on the lattice constant. The decrease of the dielectric constants with increasing pressure is due to the more increase of the second term than the increase of the first one.

It may be suggested that the increase of the pressure dependence of the dielectric constants in irradiated crystals and the decrease of that in activated crystals are ascribed to the quantity of the increase of the second term.

Infrared absorption A remarkable absorption band at around 3595 cm^{-1} is shown in LiF crystals grown in air furnace. The band is very much weaker in the crystals grown in vacuum furnace, but does not vanish perfectly. It is surmised that the 3595 cm^{-1} band is caused by F—H or O—H stretching vibration in a complex with hydrogen bonds of F—H...F or O—H...O anions, which are produced by the hydrolysis of LiF salt in the crystals⁹⁾.

When LiF crystals with the 3595 cm^{-1} band are exposed to γ -rays, the changes of the infrared absorptions are detected. Fig. 11 shows the infrared absorption spectra of LiF crystal before and after the exposures of $1.7 \times 10^6 \text{ r}$ and $4.4 \times 10^6 \text{ r}$ of γ -rays. The 3595 cm^{-1} band diminished and then finally vanished perfectly, but on the other hand a weak absorption band is enhanced at around 1950 cm^{-1} with increasing dosage of γ -rays. The both bands show a quantitative change by a finite dosage of γ -rays. The phenomena are also shown by $1.5 \times 10^5 \text{ rad}$ electron exposure and by $1.1 \times 10^{16} \text{ nvt}$ neutron exposure.

The result would be considered as follows. Generally, the stretching band of hydrogen bond in a complex shifts to lower frequency with decreasing hydrogen bond length. The large frequency displacement and the breadth of the bands are shown by the coordination of a complex with hydrogen bond to a metal¹⁰⁾. The irradiation produces free anions as the result of breaking of the complex with hydrogen bonds which contribute to the 3595 cm^{-1} band, and on the other hand

8) J. Yamashita, *Prog. Theor. Phys.*, 8, 280 (1952); 12, 454 (1954)

9) S. S. Ballard, L. S. Combes, and K. A. McCarthy, *J. Opt. Soc. Am.*, 41, 772 (1951)

10) R. C. Lord and R. E. Merrifield, *J. Chem. Phys.*, 21, 166 (1953)

The Effect of Pressure on the Defects in Alkali Halide Crystals

51

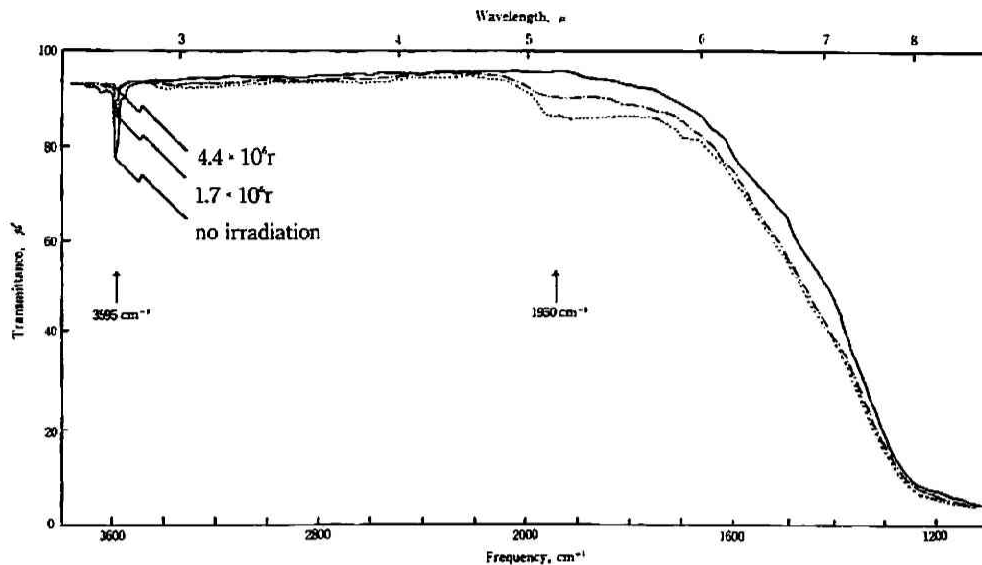


Fig. 11 The effect of γ -rays irradiation on the infrared absorption in LiF crystal

produces lithium metal and another impurity metal as the result of electron capture by metal ions. The free anions coordinate to the metal and precipitate a new complex, such as metal- $(\text{HF}_2)_n$. The short and strong hydrogen bonds are constituted in the new complex and the stretching vibration contributes to the broad band at around 1950 cm^{-1} .

*The Laboratory of Physical Chemistry,
Kyoto University*